

Suppression of static ZZ interaction in an all-transmon quantum processor

Peng Zhao,^{1,*} Dong Lan,¹ Peng Xu,² Guangming Xue,³ Mace Blank,¹ Xinsheng Tan,^{1,†} Haifeng Yu,³ and Yang Yu¹

¹*National Laboratory of Solid State Microstructures, School of Physics, Nanjing University, Nanjing 210093, China*

²*Institute of Quantum Information and Technology, Nanjing University of Posts and Telecommunications, Nanjing, Jiangsu 210003, China*

³*Beijing Academy of Quantum Information Sciences, Beijing 100193, China*

(Dated: November 10, 2020)

The superconducting transmon qubit is currently a leading qubit modality for quantum computing, but gate performance in quantum processor with transmons is often insufficient to support running complex algorithms for practical applications. It is thus highly desirable to further improve gate performance. Due to the weak anharmonicity of transmon, a static ZZ interaction between coupled transmons commonly exists, undermining the gate performance, and in long term, it can become performance limiting. Here we theoretically explore a previously unexplored parameter region in an all-transmon system to address this issue. We show that an experimentally feasible parameter region, where the ZZ interaction is heavily suppressed while leaving XY interaction with an adequate strength to implement two-qubit gates, can be found in an all-transmon system. Thus, two-qubit gates, such as cross-resonance gate or iSWAP gate, can be realized without the detrimental effect from static ZZ interaction. To illustrate this, we show that an iSWAP gate with fast gate speed and dramatically lower conditional phase error can be achieved. Scaling up to large-scale transmon quantum processor, especially the cases with fixed coupling, addressing error, idling error, and crosstalk that arises from static ZZ interaction could also be heavily suppressed.

I. INTRODUCTION

The transmon qubit has been demonstrated as a leading superconducting qubit modality for quantum computing since it has been largely responsible for the recent impressive achievements in superconducting quantum information processing [1–3]. These achievements crucially rely on the improvement of the gate performance through increasing the transmon coherence time [4] and mitigating coherent error from non-ideal parasitic interaction [5–8]. Nonetheless, state-of-the-art gate performance in transmon quantum processor so far is probably insufficient to demonstrate quantum advantage for practical applications [9] and to achieve the long-term goals of fault-tolerant quantum computing [10]. This indicates that considerable effort devoted to improving gate performance is still required.

Despite the benefit of the reproducibly long coherence times, the weak anharmonicity of the transmon currently poses a significant challenge to further improve gate performance. For single qubit gates, due to the weak anharmonicity, higher-energy levels of transmon can be easily populated during microwave driven gate operation, causing leakage error. By using the Derivative Removal by Adiabatic Gate (DRAG) scheme [11, 12], this issue can be substantially mitigated without sacrificing the gate speed, and single qubit gate with fidelity in excess of 99.9% can be achieved [1, 4]. However, various pending challenges for pursuing two-qubit gates with fast speed and high fidelity still exist due to the non-ideal parasitic interaction that arise from the weak anharmonicity of transmon [13, 14]. One of the leading non-ideal parasitic interaction is the static ZZ interaction, that is caused by the coupling between qubit state and non-qubit state

[15, 16]. This interaction has been shown to undermine the performance of XY interaction based two-qubit gates, such as Cross-Resonance gate or iSWAP gate [2, 7, 8]. Meanwhile, its residual can cause idling error, and produce quantum crosstalk related to neighboring spectator qubits [17–20], that is particularly harmful for implementing parallel gate operations and performing quantum error-correction [25]. Hopefully, these idling errors and quantum crosstalk can be strongly suppressed by using a tunable coupler [6, 21–23]. However, mitigation of static ZZ interaction for XY-based two-qubit gate operations or qubit architecture with fixed inter-qubit coupling is still an outstanding challenge for the transmon quantum processor [24].

In this work, we show that suppression of static ZZ interaction for two-qubit gate operations can be achieved by engineering quantum interference in an all-transmon quantum processor. Contrary to the commonly accepted view that for an all-transmon quantum processor, the static ZZ interaction can vanish only by turning off inter-qubit coupling [14, 24]. We find that an experimentally accessible parameter region, where static ZZ interaction is heavily suppressed while leaving XY interaction with an adequate strength to implement two-qubit gates, can be found in an all-transmon system. Because one can mitigate the detrimental effect from static ZZ interaction for two-qubit gate operations, for example, an iSWAP gate with fast speed and dramatically lower conditional phase error can be achieved. Moreover, for transmon quantum processor with fixed coupling, the idling error and quantum crosstalk arise from static ZZ coupling should also be heavily suppressed.

II. SYSTEM HAMILTONIAN

Since a superconducting qubit is naturally a multi-level system, especially for qubits with weak anharmonicity such as the transmon, its higher energy levels have non-negligible

*Electronic address: shangniguo@sina.com

†Electronic address: meisen0103@163.com

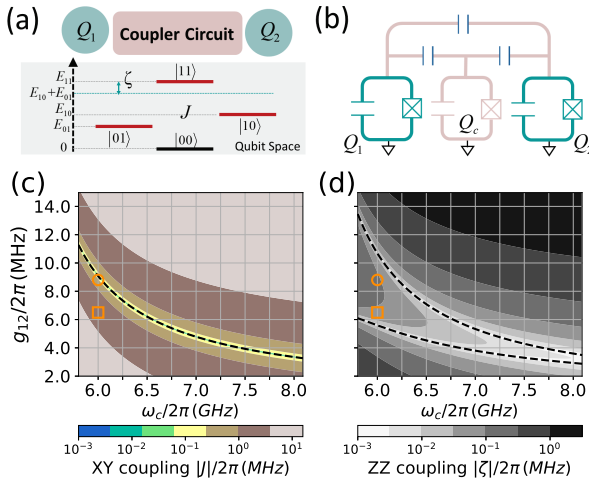


FIG. 1: (a) Circuit layout and level diagram of a coupled two-qubit system where qubits are coupled through a coupler circuit. Truncation to qubit space gives rise an effective two-qubit Hamiltonian with an inter-qubit XY coupling J and a static ZZ coupling ζ . (b) Example circuit diagram of two transmons coupled via a capacitor and a coupler [6]. (c) Landscapes of XY coupling J and (d) ZZ coupling ζ as a function of direct coupling strength g_{12} and coupler frequency ω_c in the two-transmon system (b) with qubit frequency $\omega_{1(2)}/2\pi = 5.114$ (4.914) GHz, qubit anharmonicity $\alpha_{1(2)}/2\pi = -330$ MHz, coupler anharmonicity $\alpha_c/2\pi = 0$ MHz (linear coupler), and transmon-coupler coupling strength $g_{1(2)}/2\pi = 98$ (83) MHz [7, 28]. The dashed curves in (c) and (d) correspond to contours of $J = 0$ and $\zeta = 0$, respectively. The open circle (square) in (c,d) mark the set of parameters chosen to suppress the XY (ZZ) coupling.

contribution to the inter-qubit coupling. For coupled transmons as shown in Fig. 1(a), truncation to the (computational) qubit space gives rise an effective two-qubit Hamiltonian with not only an inter-qubit XY coupling J but also a static ZZ coupling ζ (the lower panel of Fig. 1(a)) from the coupling among the higher energy levels of transmons or coupler [16]. Here, in order to achieve the suppression of this ZZ coupling for XY-based two qubit gates, we consider the all-transmon system schematically depicted in Fig. 1(b), where transmons are coupled through a coupling circuit combing a third ancilla transmon (coupler) and a capacitor. The full system can be modeled by three coupled weakly anharmonic oscillators [25], and described by (hereafter $\hbar = 1$)

$$H = \sum_j \left[\tilde{\omega}_j q_j^\dagger q_j + \frac{\alpha_j}{2} q_j^\dagger q_j^\dagger q_j q_j \right] + \sum_{j,k} g_{jk} (q_j^\dagger q_k + q_j q_k^\dagger), \quad (1)$$

where the subscript $j = 1, 2, c$ labels transmon Q_j with anharmonicity α_j and bare qubit frequency $\tilde{\omega}_j$, q_j (q_j^\dagger) is the associated annihilation (creation) operator, and g_{jk} ($j, k = 1, 2, c$) denotes strength of the coupling between Q_j and Q_k .

When both the two transmons are coupled dispersively to the coupler, i.e., the transmon-coupler detuning $|\Delta_{1(2)}| = |\tilde{\omega}_{1(2)} - \tilde{\omega}_c|$ is far larger than the transmon-coupler coupling

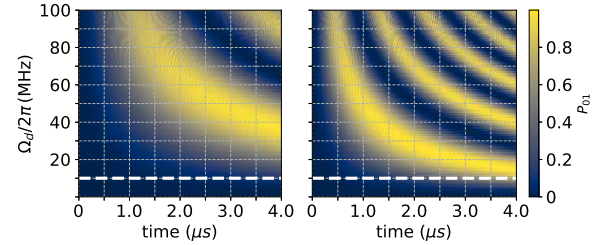


FIG. 2: Cross-resonance oscillation of target transmon Q_2 with the controlled transmon Q_1 in its ground state. (Left/right panel) Population oscillation for target transmon Q_2 as a function of strength Ω_d of the driving applied on transmon Q_1 and time with parameter set (g_{12}, ω_c) marked with open circle/square shown in Figs. 1(c,d). The other system parameters are similar to those used in Fig. 1. The horizontal dashed lines indicates the driving strength $\Omega/2\pi = 10$ MHz that is used to infer the effective XY coupling strength J [28].

strength $g_{1c(2c)}$, the system Hamiltonian in Eq. (1) can be approximated by an effective two-qubit Hamiltonian that has the following form (truncation to the qubit space)

$$H = \omega_1 \frac{ZI}{2} + \omega_2 \frac{IZ}{2} + J \frac{XX + YY}{2} + \zeta \frac{ZZ}{4}, \quad (2)$$

where (X, Y, Z, I) denote the Pauli operators and identity operator, and the order indexes the qubit number, and ω_1 (ω_2) represents the dressed qubit frequency of Q_1 (Q_2). The last two terms corresponds to the effective XY coupling with strength J and ZZ coupling with strength ζ , respectively. The XY coupling results from the direct coupling g_{12} and the coupler-mediated indirect coupling, and its strength can be approximated by [6]

$$J = g_{12} - \frac{g_{1c}g_{2c}}{2} \left(\frac{1}{\Delta_1} + \frac{1}{\Delta_2} - \frac{1}{\Sigma_1} - \frac{1}{\Sigma_2} \right), \quad (3)$$

where $\Sigma_{1(2)} = \tilde{\omega}_{1(2)} + \tilde{\omega}_c$; The ZZ coupling strength is defined as $\zeta = (E_{11} - E_{10}) - (E_{01} - E_{00})$, where E_{mn} denotes the energy of the qubit eigenstate $|mn\rangle$ ($m, n = \{0, 1\}$), and it can be obtained approximately by using perturbation theory [26, 27].

III. SUPPRESSION OF STATIC ZZ INTERACTION FOR OFF-RESONANTLY COUPLED TRANMONS

As already mentioned before, the presence of the static ZZ coupling can undermine the gate performance in transmon quantum processor. In general, the static ZZ interaction can be suppressed by turning off inter-qubit coupling. However, an inter-qubit coupling is definitely needed to implement two-qubit gates. Keeping this in mind, we must explore the possibility of relaxing this restriction in the parameter space of the present system. Figures. 1(c) and 1(d) show J (Eq. 3) and ζ (fourth-order perturbation result [26, 27]) as a function of

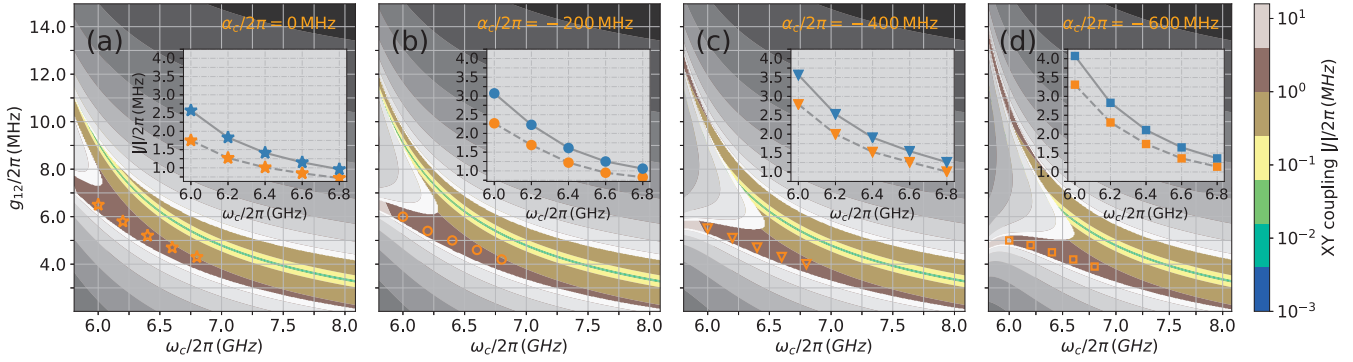


FIG. 3: Landscapes of XY coupling J (Eq. 3) and ZZ coupling ζ (numerical diagonalization) as a function of direct coupling strength g_{12} and coupler frequency ω_c with coupler anharmonicity (a) $\alpha_c = 0$ (linear coupler), (b) $\alpha_c = -200$ MHz, (c) $\alpha_c = -400$ MHz, and (d) $\alpha_c = -600$ MHz. The other system parameters are similar to those used in Fig. (1). For each coupler anharmonicity, the two landscapes are shown in single panel, and the date point in the landscape of ZZ coupling with ζ below 20 KHz is removed. The Insets of (a-d) show the maintained XY coupling strength obtained with the corresponding parameter set marked in (a-d). The solid (dashed) line represents the result derived from Eq. 3 (the period T of the simulated cross-resonance oscillation, as shown in Fig. (2)).

direct coupling strength g_{12} and coupler frequency ω_c with qubit frequency $\omega_{1(2)}/2\pi = 5.114(4.914)$ GHz, anharmonicity $\alpha_{1(2)}/2\pi = -330$ MHz, $\alpha_c/2\pi = 0$ MHz (linear coupler), and transmon-coupler coupling strength $g_{1(2)}/2\pi = 98(83)$ MHz [7, 28]. One can find that in the parameter space of (g_{12}, ω_c) , zero-point for XY coupling forms a single branch (dashed line in Fig. 1(c)). Interestingly, for case of ZZ coupling (dashed line in Fig. 1(d)), there are two separated branches. The upper one almost coexists with the zero-XY branch on the same parameter region, conforming the commonly accepted view, i.e., the static ZZ interaction can be suppressed by turning off inter-qubit coupling. However, the presence of the lower branch shows that the ZZ coupling can be heavily suppressed without the need for suppressing the XY coupling. Thus, for a system operating on the lower branch region, one can mitigate the ZZ interaction for implementing XY-based two-qubit gates.

In order to numerically verify the above results, we consider two sets of parameters, i.e., $(6.0, 6.5)$ and $(6.0, 8.8)$, as shown in Figs. 1(c,d), which mark the set of parameters chosen to suppress the XY and ZZ coupling, respectively. The ZZ coupling strength can be exactly obtained by numerical diagonalization of the full system Hamiltonian in Eq. 1, giving rise the ZZ coupling strength of $|\zeta|/2\pi = 3.9$ (3.3) KHz for the two parameter sets. To derive the XY coupling, we note that the effective XY coupling is not perfectly well-defined for present system with off-resonantly coupled transmons. Thus, here the XY coupling strength is estimated from the period T of the simulated cross-resonance oscillation (Fig. 2) with the controlled qubit Q_1 in its ground state. In the weak-drive limit, the period T can be well approximated by $2\pi/T = J\Omega_d/\Delta_{12}$ [28], where Ω_d denotes strength of the driving applied on the transmon Q_1 , and $\Delta_{12} = \omega_1 - \omega_2$ is the transmon-transmon detuning. As such, here we take $\Omega/2\pi = 10$ MHz, and the estimated XY coupling strength are $J/2\pi = 1.75$ (0.63) MHz. Thus, one can conclude that

for systems operating on the lower branch region in Fig. 1(d), the ZZ coupling can be strongly suppressed without the need for suppressing the XY coupling heavily. However, while the ZZ coupling is indeed strongly suppressed, the strength of the maintained XY coupling (here is 1.75 MHz) is too weak to support implementing a successful two-qubit gate, such as the cross-resonance gate [29].

To increase the strength of the maintained XY coupling, we consider replacing the linear coupler with an ancilla transmon coupler. Figures 3(a-d) show the ZZ coupling strength (numerical diagonalization, the date point with ZZ coping strength below 20 KHz is removed) and the XY coupling strength (Eq. 3) as a function of direct coupling strength g_{12} and coupler frequency ω_c with coupler anharmonicity $\alpha/2\pi = \{0, -200, -400, -600\}$ MHz. The other parameters are same to those used in Fig. 1. In Fig. 3, in order to easily identify the desired parameter region, i.e., suppressing the ZZ coupling while leaving XY coupling with an adequate strength to implement two-qubit gates, for each coupler anharmonicity, the associated two landscapes (ZZ and XY) are shown in a single panel. One can find that by increasing the magnitude of the coupler anharmonicity, the upper branch for suppressing ZZ coupling is shifted upward, while the lower branch is shifted downward. As result of this shift, we find that in the lower branch, the maintained XY coupling is increased by increasing $|\alpha_c|$, as shown in the inset of Fig. 3, where each date point is obtained with the parameter set marked in Fig. 3, and the solid (dashed) line corresponds to the result derived from Eq. 3 (the period T of the simulated cross-resonance oscillation). Thus, by using the transmon coupler, the residual ZZ coupling below 20 KHz and the strength of maintained XY coupling in excess of 2 MHz should be assessed experimentally for implementing cross-resonance gate with current fabrication technology [30, 31]. We note that the maintained XY coupling may further increase by optimizing the full system parameters (here we only con-

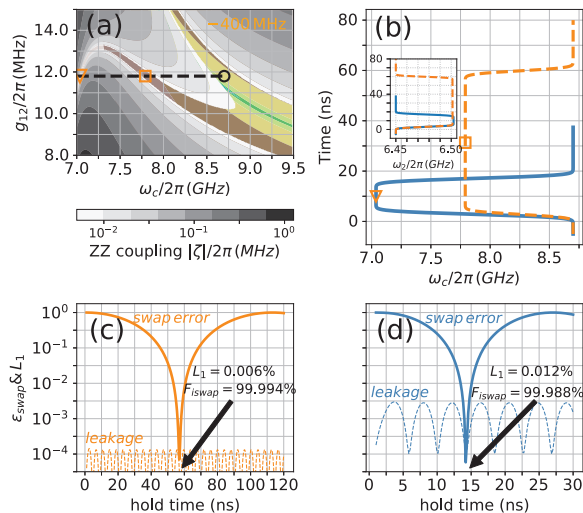


FIG. 4: (a) Landscapes of numerically calculated XY coupling strength J and ZZ coupling strength ζ (date point with ZZ coping strength below 20 KHz is removed) as a function of direct coupling strength g_{12} and coupler frequency ω_c in the two-transmon system (Fig. 1) with qubit frequency $\omega_{1(2)}/2\pi = 6.5$ GHz, qubit anharmonicity $\alpha_{1(2)}/2\pi = -250$ MHz, coupler anharmonicity $\alpha_c/2\pi = -400$ MHz, and frequency-dependent transmon-coupler coupling strength $g_{1(2)}/2\pi = 125\sqrt{\omega_c/\omega_1}$ ($130\sqrt{\omega_c/\omega_2}$) MHz. The parameter set marked by an open circle denotes the idling frequency point for the coupler, and the dashed line indicates the direct coupling strength adopted for mitigating the leakage during the iSWAP gate operation. (b) Typical control pulse for implementing an iSWAP gate, where the full width at half maximum is defined as hold time. The dashed (solid) line shows the control pulse for system operated in dispersive (quasi-dispersive) regime, marked by the open square (triangle) in (a). (c), (d) Swap error $\varepsilon_{\text{swap}}$ and leakage L_1 as a function of hold time.

sider the parameter space defined by direct coupling strength, coupler frequency, and coupler anharmonicity).

IV. SUPPRESSION OF STATIC ZZ INTERACTION FOR ON-RESONANTLY COUPLED TRANSMONS

Having shown the suppression of ZZ coupling for the off-resonantly coupled case, we now turn to consider the on-resonance case. We still consider the all-transmon system schematically depicted in Fig. 1(b), and its dynamics is full captured by the full system Hamiltonian given in Eq. 1. Fig. 4(a) shows the numerically calculated ZZ coupling strength ζ (date point with ZZ coping strength below 20 KHz is removed) and XY coupling strength J (extracted as half the energy difference between the eigenstate $|10\rangle$ and $|01\rangle$) as a function of direct coupling strength g_{12} and coupler frequency ω_c with qubit frequency $\omega_{1(2)}/2\pi = 6.5$ GHz, qubit anharmonicity $\alpha_{1(2)}/2\pi = -250$ MHz, coupler anharmonicity $\alpha_c/2\pi = -400$ MHz, and frequency-dependent transmon-coupler coupling strength $g_{1(2)}/2\pi =$

$125\sqrt{\omega_c/\omega_1}$ ($130\sqrt{\omega_c/\omega_2}$) MHz [32]. Similar to that of the off-resonantly coupled case, the zero-ZZ points for on-resonance coupled transmons also form two branches in the parameter space (g_{12}, ω_c) , where the lower branches allow us to mitigate ZZ coupling for on-resonance XY coupling based two-qubit gates.

To illustrate this, we consider the implementation of an iSWAP gate in present system with diabatic scheme [15, 32], and in order to mitigate leakage, in the following discussion, the direct coupling strength g_{12} are chosen to achieve the full synchronization between the swap and leakage error channels [32]. During the gate operations, the frequency of the Transmon Q_1 stays fixed at 6.50 GHz, while the frequencies of coupler Q_c and transmon Q_2 vary from the their idle frequency point $(\omega_{c(2)})/2\pi = 8.70$ (6.45) GHz, where both the XY and ZZ coupling are strongly suppressed) to their interaction frequency point and then come back according to the Gaussian flat-top pulse with a fixed rise/fall time of 5.66 ns, as shown in Fig. 4(b) [33]. Firstly, we consider that the system operates in the dispersive regime, and the interaction frequencies of coupler Q_c takes $\omega_c/2\pi \approx 7.90$ GHz, marked by the open square in Fig. 4(a), and the associated control pulse is shown as the dashed line in Fig. 4(b). Fig. 4(c) shows the swap error $\varepsilon_{\text{swap}} = 1 - P_{01}$ (P_{01} denotes the population in $|01\rangle$) after the time evolution for system initialized in $|10\rangle$) and the leakage L_1 [34, 35] as function of the hold time that is defined as the time-interval between the midpoints of the ramps [33]. One can find that an iSWAP gate with an intrinsic state-average gate fidelity [36] of 99.994% and leakage L_1 below 0.006% can be achieved with a hold time of 57 ns. Moreover, by extracting conditional phase error δ_θ , we find that the δ_θ is suppressed below 0.001 rad, comforting the strong suppression of the ZZ coupling. In Fig. 4(c), we also show the result for the system operated in the quasi-dispersive regime, and the control pulse is shown as the solid line in Fig. 4(b), where the interaction frequency for the coupler takes $\omega_c/2\pi \approx 7.04$ GHz (also marked by the open circle in Fig. 4(a)), giving the $g_{1c(2c)}/\Delta_{1(2)} \approx 1/4$. Although operating in the quasi-dispersive regime, an iSWAP gate with fidelity above 99.988% and leakage L_1 below 0.012% can still be achieved with a hold time of 14.3 ns. The extracted conditional phase error δ_θ is suppressed below 0.003 rad. Overall, these results indicate that the ZZ coupling can be heavily suppressed while leaving XY coupling with an adequate strength to realize a fast iSWAP gate.

V. CONCLUSION

In summary, we have demonstrated that a feasible parameter region, where the ZZ interaction is heavily suppressed while leaving XY interaction with an adequate strength to implement two-qubit gates, such as cross-resonance gate or iSWAP gate, can be found in an all-transmon system. We further show that an iSWAP gate with fast gate speed and dramatically low conditional phase error can indeed be achieved in this parameter region. Without the detrimental effect from the static ZZ coupling, for transmon quantum processor with

fixed coupling, single-qubit addressing error, idling error, and crosstalk that arise from static ZZ interaction should also be heavily suppressed. Although our demonstration is carried out on the all-transmon system where transmons are coupled through a coupler circuit combing a capacitor and an ancillary transmon coupler, one may reasonably estimate that it is also possible to achieve the mitigation of static ZZ coupling for XY-based two-qubit gates with another type of coupler circuit [23]. It is worth mentioning that in the present work, our discussion is restricted on all-transmon system where qubits are in the straddling regime [23], i.e., transmon-tranmson detuning is smaller than the magnitude of transmon anharmonicity. For transmons out of straddling regime, the previous numerical result does not show any possibility for achieving mitigation of static ZZ coupling in all-transmon device operated in a reasonable coupling regime [23, 27].

We note that in preparation of this manuscript, we were made aware of similar work performed in Ref.[37] for mitigating static ZZ coupling for implementing a ZZ-free iSWAP

gate.

Acknowledgments

We thank Ji Chu for insightful discussions. This work was partly supported by the National Key Research and Development Program of China (Grant No.2016YFA0301802), the National Natural Science Foundation of China (Grant No.61521001, and No.11890704), and the Key R&D Program of Guangdong Province (Grant No.2018B030326001). P. X. acknowledges the supported by Scientific Research Foundation of Nanjing University of Posts and Telecommunications (NY218097), NSFC (Grant No.11847050), and the Young fund of Jiangsu Natural Science Foundation of China (Grant No.BK20180750). H. Y. acknowledges support from the Beijing Natural Science Foundation (Grant No.Z190012).

[1] R. Barends, J. Kelly, A. Megrant, A. Veitia, D. Sank, E. Jeffrey, T. C. White, J. Mutus, A. G. Fowler, B. Campbell, Y. Chen, Z. Chen, B. Chiaro, A. Dunsworth, C. Neill, P. O’Malley, P. Roushan, A. Vainsencher, J. Wenner, A. N. Korotkov, A. N. Cleland, and J. M. Martinis, Superconducting quantum circuits at the surface code threshold for fault tolerance, *Nature* **508**, 500 (2014).

[2] F. Arute, K. Arya, R. Babbush, D. Bacon, J. C. Bardin, R. Barends, R. Biswas, S. Boixo, F. G. Brandao, D. A. Buell *et al.*, Quantum supremacy using a programmable superconducting processor, *Nature* **574**, 505 (2019).

[3] P. Jurcevic, A. Javadi-Abhari, L. S. Bishop, I. Lauer, D. F. Bogorin *et al.*, Demonstration of quantum volume 64 on a superconducting quantum computing system, [arXiv:2008.08571](https://arxiv.org/abs/2008.08571).

[4] M. Kjaergaard, M. E. Schwartz, J. Braumüller, P. Krantz, J. I.-J. Wang, S. Gustavsson, and W. D. Oliver, Superconducting qubits: Current state of play, [arXiv:1905.13641](https://arxiv.org/abs/1905.13641) (2019).

[5] J. M. Martinis and M. R. Geller, Fast adiabatic qubit gates using only σ_z control, *Phys. Rev. A* **90**, 022307 (2014).

[6] F. Yan, P. Krantz, Y. Sung, M. Kjaergaard, D. L. Campbell, T. P. Orlando, S. Gustavsson, and W. D. Oliver, Tunable Coupling Scheme for Implementing High-Fidelity Two-Qubit Gates, *Phys. Rev. Applied* **10**, 054062 (2018).

[7] S. Sheldon, E. Magesan, J. M. Chow, and J. M. Gambetta, Procedure for systematically tuning up cross-talk in the cross-resonance gate, *Phys. Rev. A* **93**, 060302 (2016).

[8] N. Sundaresan, I. Lauer, E. Pritchett, E. Magesan, P. Jurcevic, and J. M. Gambetta, Reducing unitary and spectator errors in cross resonance with optimized rotary echoes, [arXiv:2007.02925](https://arxiv.org/abs/2007.02925).

[9] J. Preskill, Quantum Computing in the NISQ era and beyond, *Quantum* **2**, 79 (2018).

[10] A. G. Fowler, M. Mariantoni, J. M. Martinis, and A. N. Cleland, Surface codes: Towards practical large-scale quantum computation, *Phys. Rev. A* **86**, 032324 (2012).

[11] F. Motzoi, J. M. Gambetta, P. Rebentrost, and F. K. Wilhelm, Simple Pulses for Elimination of Leakage in Weakly Nonlinear Qubits , *Phys. Rev. Lett.* **103**, 110501 (2009)

[12] Z. Chen, J. Kelly, C. Quintana, R. Barends, B. Campbell, Y. Chen, B. Chiaro, A. Dunsworth, A. G. Fowler, E. Lucero, E. Jeffrey, A. Megrant, J. Mutus, M. Neeley, C. Neill, P. J. J. O’Malley, P. Roushan, D. Sank, A. Vainsencher, J. Wenner, T. C. White, A. N. Korotkov, and J. M. Martinis, Measuring and Suppressing Quantum State Leakage in a Superconducting Qubit, *Phys. Rev. Lett.* **116**, 020501 (2016)

[13] P. Krantz, M. Kjaergaard, F. Yan, T. P. Orlando, S. Gustavsson, and W. D. Oliver, A quantum engineer’s guide to superconducting qubits, *Applied Physics Reviews* **6**, 021318 (2019).

[14] A. Blais, A.L. Grimsmo, S.M. Girvin and A. Wallraff, Circuit Quantum Electrodynamics, [arXiv:2005.12667](https://arxiv.org/abs/2005.12667).

[15] F. W. Strauch, P. R. Johnson, A. J. Dragt, C. J. Lobb, J. R. Anderson, and F. C. Wellstood, Quantum Logic Gates for Coupled Superconducting Phase Qubits, *Phys. Rev. Lett.* **91**, 167005 (2003).

[16] L. DiCarlo, J. M. Chow, J. M. Gambetta, L. S. Bishop, B. R. Johnson, D. I. Schuster, J. Majer, A. Blais, L. Frunzio, S. M. Girvin, and R. J. Schoelkopf, Demonstration of two-qubit algorithms with a superconducting quantum processor, *Nature (London)* **460**, 240 (2009).

[17] D. C. McKay, S. Sheldon, J. A. Smolin, J. M. Chow, and J. M. Gambetta, Three Qubit Randomized Benchmarking, *Phys. Rev. Lett.* **122**, 200502 (2019).

[18] M. Takita, A. D. Córcoles, E. Magesan, B. Abdo, M. Brink, A. Cross, J. M. Chow, and J. M. Gambetta, Demonstration of Weight-Four Parity Measurements in the Surface Code Architecture, *Phys. Rev. Lett.* **117**, 210505 (2016).

[19] C. C. Bultink, T. E. O’Brien, R. Vollmer, N. Muthusubramanian, M. W. Beekman, M. A. Rol, X. Fu, B. Tarasinski, V. Ostroukh, B. Varbanov, A. Bruno, L. DiCarlo, Protecting quantum entanglement from qubit errors and leakage via repetitive parity measurements, [arXiv:1905.12731](https://arxiv.org/abs/1905.12731) (2020).

[20] S. Krinner, S. Lazar, A. Remm, C.K. Andersen, N. Lacroix, G.J. Norris, C. Hellings, M. Gabureac, C. Eichler, and A. Wallraff, Benchmarking Coherent Errors in Controlled-Phase Gates due to Spectator Qubits, *Phys. Rev. Applied* **14**, 024042 (2020).

[21] Y. Chen, C. Neill, P. Roushan, N. Leung, M. Fang, R. Barends, J. Kelly, B. Campbell, Z. Chen, B. Chiaro, A. Dunsworth, E. Jeffrey, A. Megrant, J. Y. Mutus, P. J. J. O’Malley, C.

M. Quintana, D. Sank, A. Vainsencher, J. Wenner, T. C. White, M. R. Geller, A. N. Cleland, and J. M. Martinis, Qubit architecture with high coherence and fast tunable coupling, *Phys. Rev. Lett.* **113**, 220502 (2014).

[22] C. Neill. A path towards quantum supremacy with superconducting qubits. PhD thesis, University of California Santa Barbara, Dec 2017.

[23] P. S. Mundada, G. Zhang, T. Hazard, and A. A. Houck, Suppression of Qubit Crosstalk in a Tunable Coupling Superconducting Circuit, *Phys. Rev. Applied* **12**, 054023 (2019).

[24] X. Xu and M.H. Ansari, ZZ freedom in two qubit gates, [arXiv:2009.00485](https://arxiv.org/abs/2009.00485).

[25] J. Koch, T. M. Yu, J. Gambetta, A. A. Houck, D. I. Schuster, J. Majer, A. Blais, M. H. Devoret, S. M. Girvin, and R. J. Schoelkopf, Charge-insensitive qubit design derived from the cooper pair box, *Phys. Rev. A* **76**, 042319 (2007).

[26] Li, T. Cai, H. Yan, Z. Wang, X. Pan, Y. Ma, W. Cai, J. Han, Z. Hua, X. Han, Y. Wu, H. Zhang, H. Wang, Yipu Song, Luming Duan, and Luyan Sun, Tunable Coupler for Realizing a Controlled-Phase Gate with Dynamically Decoupled Regime in a Superconducting Circuit, *Phys. Rev. Applied* **14**, 024070 (2020).

[27] J. Chu *et al.*, in preparation. (2020).

[28] E. Magesan and J. M. Gambetta, Effective Hamiltonian models of the cross-resonance gate, *Phys. Rev. A* **101**, 052308 (2020).

[29] F. Solgun, D. DiVincenzo, and J. Gambetta, Simple Impedance Response Formulas for the Dispersive Interaction Rates in the Effective Hamiltonians of Low Anharmonicity Superconducting Qubits, *IEEE Trans. Microw. Theory Tech.* **67**, 928 (2019).

[30] J M Kreikebaum, K P O'Brien, A. Morvan, and I Siddiqi, Improving wafer-scale Josephson junction resistance variation in superconducting quantum coherent circuits, *Supercond. Sci. Technol.* **33**, 06LT02 (2020).

[31] J. B. Hertzberg, E. J. Zhang, S. Rosenblatt, E. Magesan, J. A. Smolin, J.-B. Yau, V. P. Adiga, M. Sandberg, M. Brink, J. M. Chow, and J. S. Orcutt, Laser-annealing Josephson junctions for yielding scaled-up superconducting quantum processors, [arXiv:2009.00781](https://arxiv.org/abs/2009.00781).

[32] R. Barends, C. M. Quintana, A. G. Petukhov, Y. Chen, D. Kafri, K. Kechedzhi *et al.*, Diabatic Gates for Frequency-Tunable Superconducting Qubits, *Phys. Rev. Lett.* **123**, 210501 (2019).

[33] J. Ghosh, A. Galiautdinov, Z. Zhou, A. N. Korotkov, J. M. Martinis, and M. R. Geller, High-fidelity controlled- σ^Z gate for resonator-based superconducting quantum computers, *Phys. Rev. A* **87**, 022309 (2013).

[34] C. J. Wood and J. M. Gambetta, Quantification and characterization of leakage errors, *Phys. Rev. A* **97**, 032306 (2018).

[35] M. A. Rol, F. Battistel, F. K. Malinowski, C. C. Bultink, B. M. Tarasinski, R. Vollmer, N. Haider, N. Muthusubramanian, A. Bruno, B. M. Terhal, and L. DiCarlo, Fast, High-Fidelity Conditional-Phase Gate Exploiting Leakage Interference in Weakly Anharmonic Superconducting Qubits, *Phys. Rev. Lett.* **123**, 120502 (2019).

[36] L. H. Pedersen, N. M. Møller, and K. Mølmer, Fidelity of quantum operations, *Phys. Lett. A* **367**, 47 (2007).

[37] Y. Sung, L. Ding, J. Braumüller, A. Vepsäläinen, B. Kannan, M. Kjaergaard, A. Greene, G. O. Samach, C. McNally, D. Kim, A. Melville, B. M. Niedzielski, M. E. Schwartz, J. L. Yoder, T. P. Orlando, S. Gustavsson, and W. D. Oliver, Realization of high-fidelity CZ and ZZ-free iSWAP gates with a tunable coupler , [arXiv:2011.01261](https://arxiv.org/abs/2011.01261).